Artur DZIUŁKO, Adam MILCZAREK, Mariusz MALINOWSKI

Warsaw University of Technology, Institute of Control and Industrial Electronics, Warsaw, Poland

doi:10.15199/48.2015.01.15

Implementation of Equal Reactive Power Sharing Algorithm in Droop-Controlled Islanded AC Microgrid

***Abstract**. This paper presents the implementation of the hierarchical control algorithm with droop method and equal reactive power sharing algorithm (ERPS) for an islanded AC microgrid. In the typical applications of microgrid the reactive power flow remains uncontrolled, what may negatively impact the efficiency of the generation unit and cause various problems to power converters. The presented solution will provide an equal reactive power generation by each source, enhancing effectiveness of each generation unit and an overall microgrid reliability and performance.*

Streszczenie. *Artykuł omawia zagadnienia implementacji hierarchicznego systemu sterowania, zawierającego metodę sterowania uchybem amplitudy i częstotliwości napięcia przekształtnika oraz algorytm równomiernego podziału mocy biernej w autonomicznej mikrosieci elektroenergetycznej AC. W klasycznej metodzie sterowania uchybem podział mocy biernej zależy od stosunku mocy czynnych poszczególnych przekształtników. Nie ma możliwości sterowania tym podziałem, co może prowadzić do przeciążenia i wyłączenia przekształtnika bądź cyrkulacji mocy biernej pomiędzy przekształtnikami. Przedstawione rozwiązanie zapewnia równy podział mocy biernej bez względu na zmieniającą się moc czynną, co eliminuje wspomniane problemy. (**Implementacja algorytmu równego podziały mocy biernej ze sterowaniem uchybem napięcia w autonomicznej mikrosieci AC**).*

Keywords: AC microgrid, equal reactive power sharing, hierarchical control, droop control.
Słowa kluczowe: mikrosieć AC, równy podział mocy biernej, sterowanie hierarchiczne, sterowanie uchybem.

Introduction

Microgrids are the most recent approach towards the electrical power generation, management and distribution. They are local power networks composed of the renewable energy sources (RES), conventional distributed generation (DG) units, energy storages and loads, which are forming an advanced system with the own control structure and communication interfaces. Microgrids usually are working in an AC or DC topology, but there are also hybrid solutions incorporating both topologies into one microgrid. Moreover, they can operate in one of the two modes: as a standalone electrical system (islanded, autonomous operation) or cooperate with the main power network [1].

In typical microgrid, RES are interconnected through power converters, which have own control algorithms and one common control unit for entire system. Many different control strategies were developed for the aforementioned microgrid topologies and modes of operation, such as the active load sharing methods (centralized control, master-slave, average load sharing) or wireless (droop method, wireless power sharing controller) [2-3].These results are creating in various solutions, which are utilized in many applications such as military, marine, aviation, automotive, domestic, rural and urban areas, remote locations with high renewable energy potential, industrial facilities.

The major task of the microgrid system is to provide an uninterruptible supply of the high quality power, better exploitation of RES and enhancement of the efficiency and performance of electrical systems. To satisfy most of these demands the reactive power flow in microgrids has to be controlled. In the typical microgrid solutions this flow is not overseen, hence the power converters may absorb or inject significant amounts of reactive power, what can decrease the converter efficiency, lead to overheating or even failures, excluding generation unit from microgrid. These may significantly reduce the microgrid reliability and performance.

In this paper, a hierarchical droop control with an equal reactive power sharing algorithm is implemented in an islanded AC microgrid in order to provide solutions for aforementioned issues.

The microgrid structure

Figure 1 presents the block scheme of the typical three-phase islanded AC microgrid. In this configuration all energy sources and storages are connected through the power converters to the main AC transmission line in a parallel configuration, usually they are equipped with the LCL filter at the output. These components are forming a single DG unit, which are finally connected in the point of common coupling (PCC). Moreover AC or DC loads with interfacing converters may be interconnected as well.

The chosen topology advantages over the DC configuration in terms of the supervisory and protection devices, which for the AC infrastructure are well developed, more advanced, efficient and cheaper. Moreover processes of planning, implementation and maintenance are easier and less costly. However there are also some issues in AC topology, such as the need for synchronization of every source before connection, the frequency deviations and reactive power flow [1]. Despite that, the synchronization can be easily performed by the modern control units through additional control loops such as phase locked loop (PLL). Nonetheless the reactive power flow is more problematic.

Consequently, the islanded mode of operation demands from a microgrid control system to oversee and fulfil several crucial tasks such as providing the general stability, regulation of voltage amplitude and frequency, ensure the appropriate power sharing, management, uninterruptible power supply.

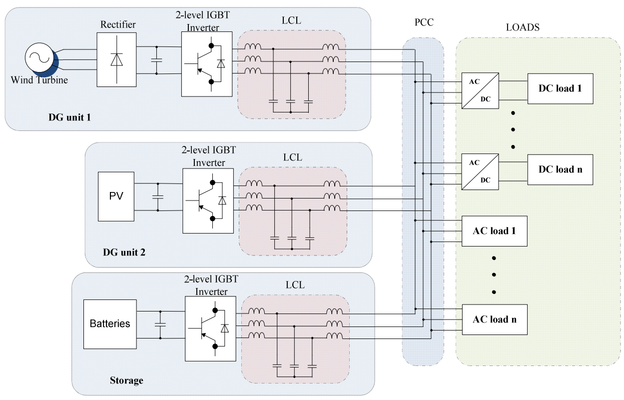

Fig. 1. Block scheme of the typical three-phase islanded AC microgrid

Microgrid control algorithm

Microgrids are advanced structures, requiring fast, efficient and robust control systems to provide stability, protection, power management, distribution, oversight of the transition states and fault detections. In order to overcome many challenges and accomplish multiple control tasks, an adequate control technique must be applied.

There are two fundamental control methods. The first one is based on active load sharing between converters, in which communication links are necessary [3]. The second contains wireless methods, which eliminate that necessity and are based on local measurements, such the droop control method [4]. For this study purpose, the developed control algorithm is based on the classical droop method. Additionally a hierarchical control approach is utilized to allow the proper active and reactive power management.

A. Hierarchical Control

Microgrids are complex systems which require control algorithms for every single DG unit and the entire structure, moreover they incorporate additional algorithms providing multiple features. To deal with numerous demands, a hierarchical approach was proposed in order to organize those algorithms in levels, where each level is responsible for different tasks. For the islanded microgrids with regard to the ISA-95 standard, three levels are implemented: secondary, primary and zero level control [5].

Level 0 is composed of the inner regulation loops of converter output voltage and current, which are in proposed solution accomplished by the proportional-resonant (PR) controllers, which allow eliminating steady state error for selected frequency and can be utilized for the harmonics compensation as well [6].

Level 1 is responsible for converter output voltage amplitude and frequency regulation. The droop method is implemented in this level.

Level 2 incorporates algorithms that regulates microgrids voltage amplitude and frequency, and manages the power sharing as well. In this study an equal reactive power sharing is implemented as secondary control level.

B. Classical Droop Control Method

The classical droop control was designed for the converters connected in parallel. It is a wireless method since it doesn't require communication links between their control units. This greatly enhances the modularity of a microgrid system allowing easy connection of additional DG units, as every single unit is equipped with the own voltage control loop.

The principle of this method is based on assumption, that by regulating the inverters output voltage amplitude and frequency droops, will allow to control the active and reactive power flow between the source and microgrid.

There are two droop strategies developed, which are adopted with regard to the character of the inverters output impedance. As the output impedance is mainly inductive due to the installed LCL filters with large inductors, the P-ω and Q-E droops are utilized and given by following equations (1) and (2) consequently [4]:

(1) $$\omega = \omega_{ref} - G_P(s) * (P - P_{ref})$$

(2) $$E = E_{ref} - G_Q(s) * (Q - Q_{ref})$$

where $G_P(s)$ and $G_Q(s)$ in classical droop method are constant coefficients, however in cooperation with the secondary level they are substituted by the proportional-integral (PI) controllers. In both solutions they are defining the steepness of P-ω and Q-E slopes (fig. 2), therefore connected inverters can inject the desire amount of active and reactive power, and of the accurate load sharing among them as well. The proposed block scheme of droop control is presented in figure 3 as primary and zero control level.

C. Equal Reactive Power Sharing Algorithm

By adopting droop control only, the complete performance of reactive power sharing among inverters cannot be achieved since reactive power strictly depends on the changing active power. Therefore a superior control level must be applied, such as secondary control with an equal reactive power sharing algorithm. It utilizes the locally measured three-phase currents and voltages of each inverter, and in the next step they are transformed into the $\alpha\beta$ stationary coordinate system by Clarke transformation [7]. The $\alpha\beta$ values are used to calculate reactive power values in following manner [8]:

(3) $$p = u_\alpha i_\alpha + u_\beta i_\beta$$

(4) $$q = u_\beta i_\alpha - u_\alpha i_\beta$$

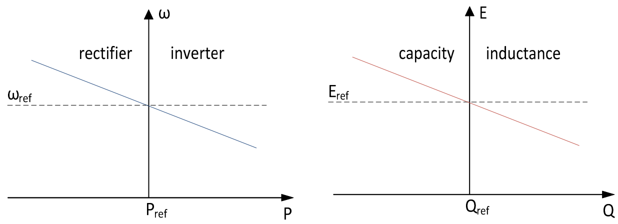

Fig. 2. Droop characteristics, from the left: frequency-active power droop, amplitude-reactive power droop

Finally reactive power reference for the k-inverter connected to the microgrid is calculated as follows:

(5) $$Q_{ref\_k} = \frac{1}{K}\sum_{k=1}^{K} q_k = \frac{Q_{total}}{K}$$

where Q_{total} is the total reactive power generated by all converters, K is the number of connected inverters to the microgrid, k – is index of converter and q_k is instantaneous value of reactive power for k-th converter.

The block scheme of proposed hierarchical control structure with droop method and equal reactive power sharing algorithm is shown in figure 3. It must be noticed, that additional communication links between the secondary controller and control units of each inverter must be applied in this approach, what is a drawback of this solution. However, accurate power sharing may be obtained, providing better exploitation of DG units in microgrid system.

Simulation study

In this section, a proposed microgrid solution has been simulated using Matlab/Simulink/Plecs software. The simulation model consisted of three identical 2-level inverters with an output LCL filter, powered by DC links, forming three DG units which were connected in parallel in PCC along with the R, RL and RLC loads. The simulation model is presented in figure 4, the electrical parameters of the filters and loads are listed in table 1.

A. ERPS Algorithm operation

First of all, an observation of the microgrid operation with an inactive ERPS control was performed and after that the operation with active ERPS is starting. Hence in the first step, microgrid was controlled only by droop method, afterwards during a steady-state operation of the system, the ERPS algorithm was turned on. Figure5 demonstrates the active and reactive powers generated by each DG unit.

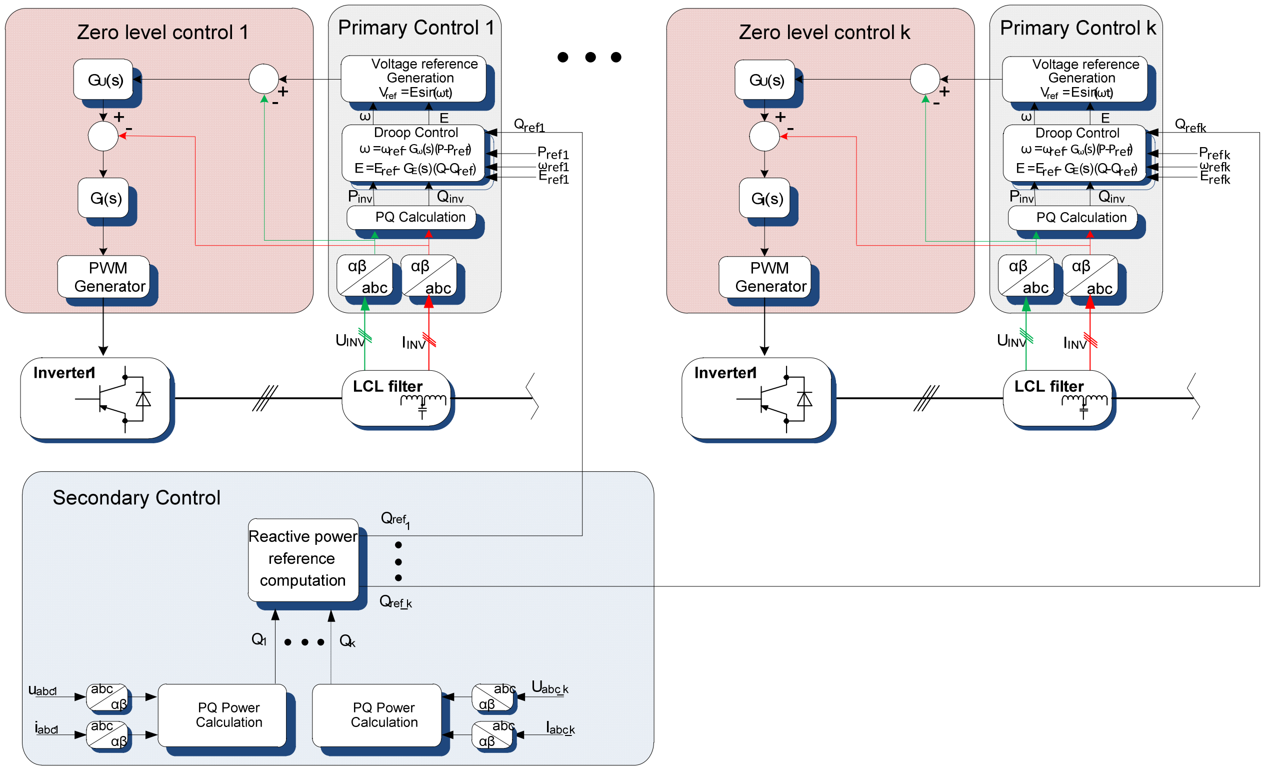

Fig. 3. Block scheme of the implemented three level control structure for an islanded AC microgrid with *k*-inverters connected

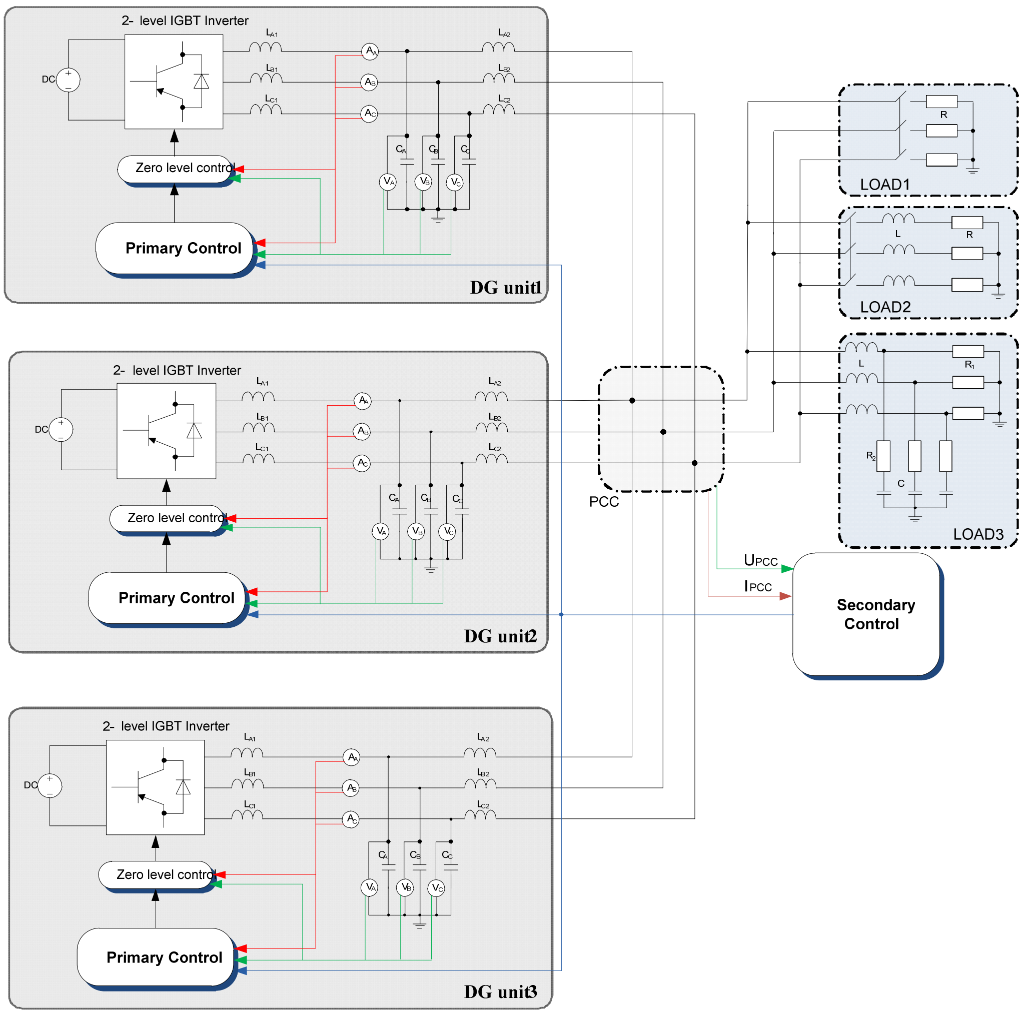

Fig. 4. Block scheme of and AC islanded microgrid simulation model with hierarchical, three level control scheme

Table 1. Electrical parameters of the simulation model power circuit

Circuit	Element	Value	Unit	Description
DG unit 1	DC link	650	V	
	L_{A1}, L_{B1}, L_{C1}	1.8	mH	LCL filter
	L_{A2}, L_{B2}, L_{C2}	1.8	mH	
	C_A, C_B, C_C	320	μF	
DG unit 2	DC link	650	V	
	L_{A1}, L_{B1}, L_{C1}	1.815	mH	LCL filter
	L_{A2}, L_{B2}, L_{C2}	1.8	mH	
	C_A, C_B, C_C	330	μF	
DG unit 3	DC link	650	V	
	L_{A1}, L_{B1}, L_{C1}	1.9	mH	LCL filter
	L_{A2}, L_{B2}, L_{C2}	1.8	mH	
	C_A, C_B, C_C	335	μF	
Load 1	R	75	Ω	
Load 2	R	65.28	Ω	
	L	0.03	H	
Load 3	R_1	50	Ω	
	R_2	250	Ω	
	L	0.3	H	
	C	500	μF	

It can be observed that the reactive power flow is different for each inverter due to the mismatch of instantaneous active powers (t = <0.3s, 0.5s>). However, after the activation of ERPS algorithm, reactive power generation is evened to the same level after transition state. Simultaneously, no significant impact on active power flow is noticed. The occurring slight deviation is due to the interdependence between both powers

Fig. 5. The active power flow (upper plot) and reactive power flow (lower plot). The P_1 and Q_1 waveforms represent first inverter active/reactive power flow, the P_2 and Q_2 for the second inverter and the P_3 and Q_3 for the third inverter, the Q_{ref} represents the reactive power reference provided by ERPS algorithm [9]

B. Varying Load Demand

To investigate the behaviour and accuracy of equal reactive power sharing algorithm, during the changing load demand, e.g. when connecting or disconnecting loads to or from microgrid, several step load changes were performed. Additionally, an unequal active power division among DG units is applied to simulate the real conditions, in which active power generation is dependent on the energy source potential and algorithms such as maximum power point tracking (MPPT). Therefore the active powers supplied by DG units in most conditions aren't equal.

Figure 6 presents the active and reactive powers of each inverter. Notice that throughout all changes that occur, the reactive power generation is maintained equal in steady-state of microgrid operation. Moreover, during the transition states in t=0.25s, t=0.5s, which are the resistive load steps and t=0.75s, which is RL load change, no significant overregulation in power flow is observed. In addition, the algorithm provides good voltage and current regulation for converters (Fig. 7).

Fig. 6. The active power flow (upper plot) and reactive power flow (lower plot). The P1 and Q1 waveforms represent first inverter active/reactive power flow, the P2 and Q2 for the second inverter and the P3 and Q3 for the third inverter [9]

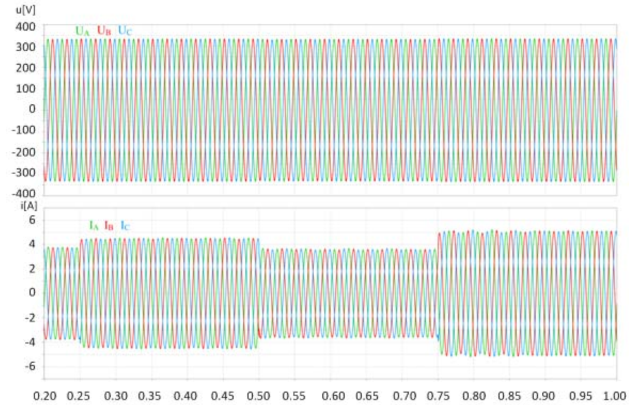

Fig. 7. Phase voltages and currents for one of converters during varying load demand [9]

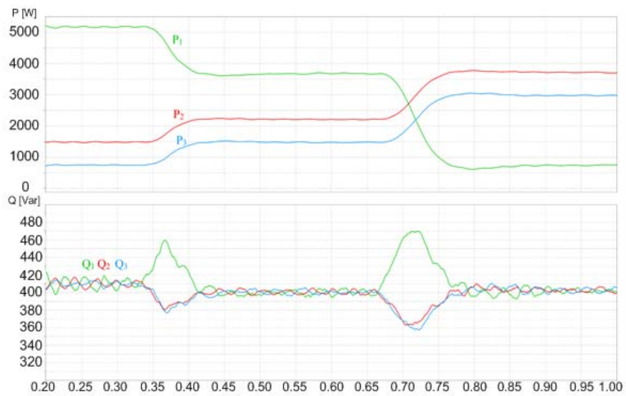

Fig. 8. The active power flow (upper plot) and reactive power flow (lower plot). The P_1 and Q_1 waveforms represent first inverter power flow, the P_2 and Q_2 for the second inverter and the P_3 and Q_3 for the third inverter [9]

C. Varying Active Power Sharing

To study the behaviour and performance of ERPS algorithm during the varying active power generation by each DG unit, several changes of the active power sharing ratio were conducted in t=0.33s and t=0.66s. Figure 8 demonstrates the active and reactive power flows. It can be observed that in steady-state of microgrid operation, reactive power generation is achieved equal. However in the transition states, when the active power generated by inverter changes, significant overregulation in reactive power flow can be noticed. Although the deviations are quickly damped by the control system, it can be considered in further investigations to adopt additional control loops like decoupling between droop control signals or the virtual impedance. Notice, that the overregulation in reactive power does not affects voltage regulation (Fig. 9).

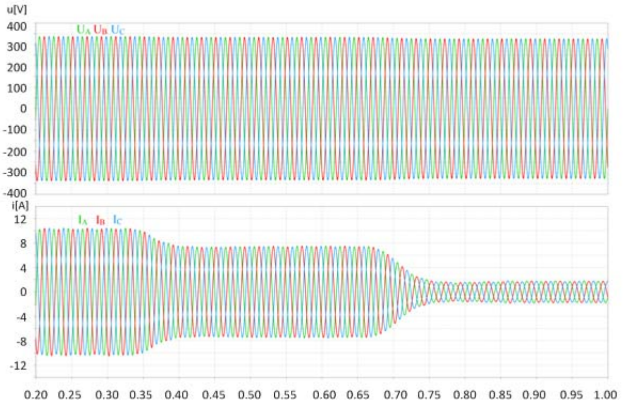

Fig. 9. Phase voltages and currents for one of converters during varying active power sharing [9]

Experimental verification

In this section, several experimental tests were conducted in order to verify the validity of the implemented equal reactive power sharing algorithm and simulation results. Therefore laboratory model was designed and built (Fig. 10). It consisted of two DG units, composed of the three-phase 2 level IGBT inverters with an output LCL filters, which were powered by the DC links. They were connected in the PCC along with the R and RL load. The list of utilized components and their ratings are presented in table 2. The control algorithm was designed in C-language and implemented on the DS1103 dSpace platform. For the experimental testing, active and reactive power waveforms were collected for three different conditions, similar to the simulation study.

Table 2. Electrical parameters of the utilized elements in the microgrid laboratory model

Circuit	Element	Value	Unit	Description
DG unit 1	Inverter 1	7.5	kVA	2-level IGBT
	$L_{A11}, L_{B11}, L_{C11}$	5	mH	LCL filter
	$L_{A12}, L_{B12}, L_{C12}$	3.24	mH	
	$C_{A11}, C_{B11}, C_{C11}$	6	μF	
DG unit 2	Inverter 2	11	kW	2-level IGBT
	$L_{A11}, L_{B11}, L_{C11}$	5	mH	LCL filter
	$L_{A12}, L_{B12}, L_{C12}$	4.28	mH	
	$C_{A11}, C_{B11}, C_{C11}$	6	μF	
Load1	R	6	Ω	
	L	2.42	mH	
Load2	R	28.3	Ω	

A. ERPS Algorithm Operation

The first test included an activation of ERPS algorithm while a steady-state of microgrid operation with droop control only. Figure 11 presents the active and reactive power generated by both inverters. It can be noticed that with droop control only, the reactive power shares unequally between units. Afterwards, the ERPS was activated and the reactive power generation is achieved equal after the transition state and maintained in the steady-state. Figure 12 shows the waveforms of voltage and currents for one of converters, proving the proper regulation of presented algorithm. Moreover, the ERPS provides corrects voltage and currents in PCC (Fig. 13).

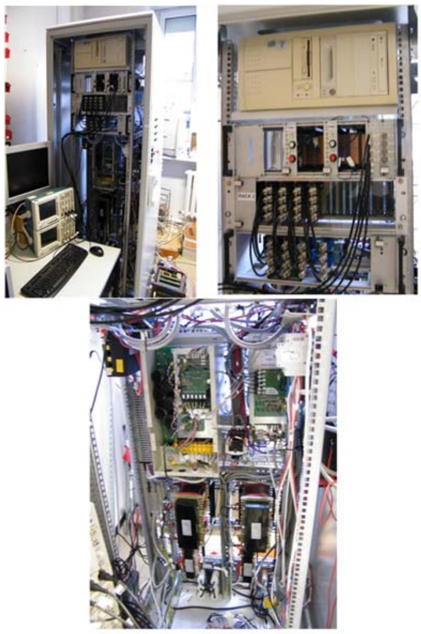

Fig. 10. Experimental setup: from the left: view of whole system, the host PC with DS1103 and current, voltage measurement cards, PWM and ADC cards, on the last one on the bottom: two power converters and two LCL filters.

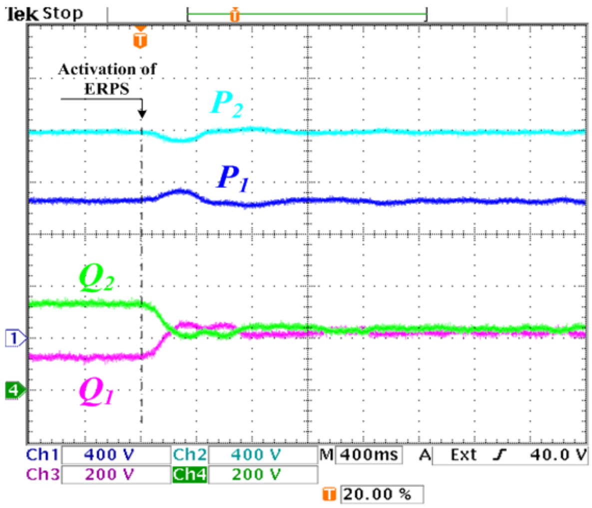

Fig. 11. The transition-state waveforms of active and reactive powers of first DG unit (P_1, Q_1), and second DG unit (P_2, Q_2), after activating the equal reactive power sharing algorithm.(P_1 and P_2 are 400 W/div, Q_1 and Q_2 are 200 Var/div) [9]

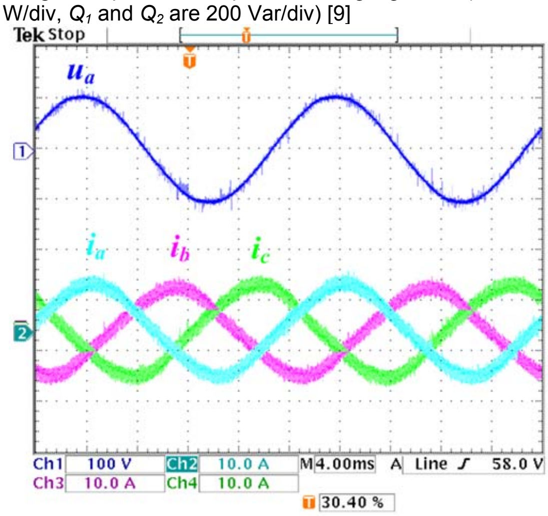

Fig. 12. The steady-state waveforms of voltage and currents of first DG unit during the equal reactive power sharing, u_a – phase voltage, i_a, i_b, i_c – phase currents.

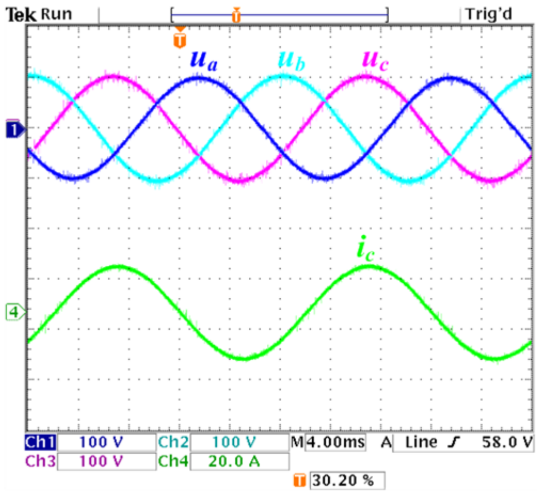

Fig. 13. The steady-state waveforms of voltages and current in PCC during the equal reactive power sharing, u_a, u_b, u_c – phase voltages, i_a – phase currents.

B. Varying Load Demand

In this part of the experimental verification, an investigation in performance of EPRS algorithm, during the step changes of the load is performed. Additionally an unequal active power division is imposed similarly as during simulation study. First of all, a disconnection of the load was conducted, and the active and reactive power waveforms are presented in fig. 14. Afterwards, a connection of the load was performed and consequently P-Q waveforms are presented in figure 15. It can be observed from the presented figures, that the proposed control algorithm manages to maintain equal reactive power generation in steady-state operation. Moreover, the occurring deviations in the transition states are insignificant and the quick ride-through is achieved.

C. Varying Active Power Generation

Similarly to the simulation study, the last part of the experimental tests involved the changing active power sharing between the DG units in order to investigate the performance of ERPS algorithm when sources change their power generation. Figure 16 shows the active and reactive power waveforms of both units during the changing ration of division from 40%/60% to 30%/70%, respectively for the first and second inverter.

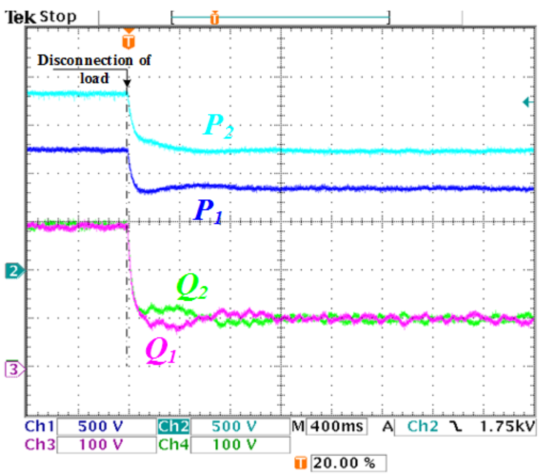

Fig. 14. The transition-state waveforms of active and reactive powers of first DG unit (P_1, Q_1), and second DG unit (P_2, Q_2), during the unequal active power division, after the disconnection of a load. (P_1 and P_2 are 500 W/div, Q_1 and Q_2 are 100 Var/div) [9]

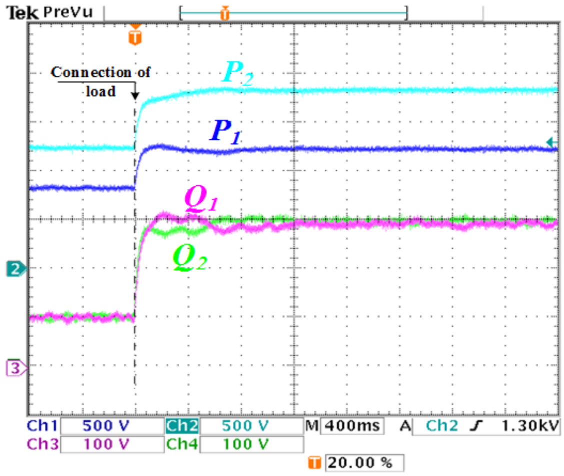

Fig. 15. The transition-state waveforms of active and reactive powers of first DG unit (P_1, Q_1), and second DG unit (P_2, Q_2), during the unequal active power division, after the connection of a load.(P_1 and P_2 are 500 W/div, Q_1 and Q_2 are 100 Var/div) [9]

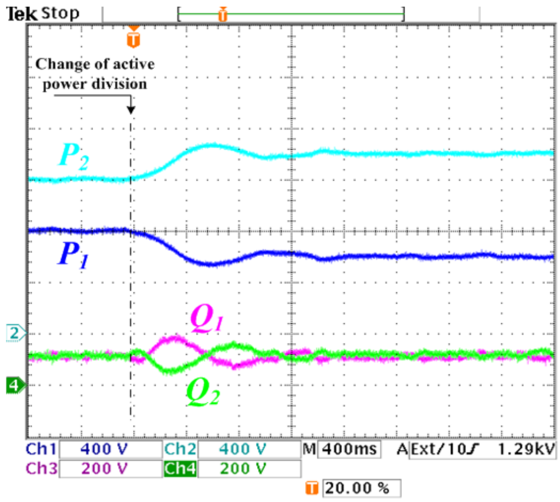

Fig. 16. The transition-state waveforms of active and reactive powers of first DG unit (P_1, Q_1), and second DG unit (P_2, Q_2), after changing the active power division ratio from 40%/60% to 30%/70%. (P_1 and P_2 are 400 W/div, Q_1 and Q_2 are 200 Var/div) [9]

As it can be observed, the results are like in the simulation. The changing active power generation takes an impact on the reactive power flow. Nonetheless the control system provides good damping and quickly achieves steady-state.

Conclusions

To minimize the circulating reactive power between inverters and the resulting negative effects which can occur, an implementation of hierarchical droop control with equal reactive power sharing algorithm has been implemented for an islanded AC microgrid.

It was presented through the simulation study and experimental tests, that utilizing proper control algorithm allows to control the power flow and achieve precise equal reactive power sharing. Consequently, better exploitation of the DG units in AC microgrid can be achieved as well as prevention of reactive power circulation between converters. Moreover the proposed solution has proven effective when different dynamic changes appear in microgrid, therefore, multiple disconnections and connections of loads can be performed, as well as sources may freely change their power generation without a concern that it will cause a threat to the system stability or to the reactive power sharing accuracy.

Presented work was partly funded by the National Science Centre granted under Decision No DEC-2013/09/N/ST7/02814 "Development and investigation of reactive power and energy storage management algorithms in smart microgrid" and partly by Department of Electrical Engineering, Warsaw University of Technology in the statute framework.

REFERENCES

[1] Loh P. C., Ding Li, Yi Kang Chai, Blaabjerg F., Autonomous Operation of Hybrid Microgrid With AC and DC subgrids, *IEEE Transactions on Power Electronics*, Vol. 28, May 2013, 2214-2223

[2] Vasquez J. C., Guerrero J. M., Miret J., Castilla M., De Vicuña L. G., Hierarchical Control of Intelligent Microgrids, *IEEEIndustrial Electronics Magazine*, Vol. 4,December 2010, 23-29

[3] Guerrero J. M., Lijun Hang, Uceda J., Control of Distributed Uninterruptible Power Supply System, *IEEE Transactions on Industrial Electronics*, Vol. 55, August 2008,2845-2859

[4] Guerrero J. M., Berbel N., Matas J., Sosa J. L., De Vicuña L. G., Droop Control Method with Virtual Output Impedance for Parallel Operation of Uninterruptible Power Supply Systems in a Microgrid, *IEEE-APEC Conference*,February-March 2007, 1126-1132

[5] Guerrero J. M., Vasquez J. C., Teodorescu R., Hierarchical Control of Droop-Controlled DC and AC Microgrids – A General Approach Towards Standarization, *IEEE-IECON Conference*, November 2009, 4305-4310

[6] Teodorescu R., Blaabjerg F., Liserre M., Loh P. C., Proportional-Resonant Controllers and Filters for Grid Connected Voltage Source Converters, *IEE Proceedings Electric Power Applications*., Vol 153, No. 5, September 2006, 750-762

[7] Duesterhoeft W. C., Schulz Jr. M. W., Clarke E., Determination of Instantaneous Currents and Voltages by Means of Alpha, Beta, and Zero Components, *IEEE Transactions of the American Institute of Electrical Engineers*, Vol. 70, no. 2, , July 1951, 1248-1255

[8] Czarnecki L. S., Instantaneous Reactive Power p-q Theory and Power Properties of Three-Phase Systems, *IEEE Transactions on Power Delivery*, Vol. 21, no. 1, 2006, 362-367

[9] Dziułko A., Development and implementation of equal reactive power sharing algorithm among PWM converters in islanded AC microgrid, *M.Sc. thesis, WUT, Institute of Control and Industrial Electronics*, May 2014.

***Authors**: mgr inż. Artur Dziułko, mgr inż. Adam Milczarek, dr hab. inż. Mariusz Malinowski, Warsaw University of Technology, Institute of Control and Industrial Electronics, ul. Koszykowa 75a, 00-662 Warszawa, e-mail: addziulko@gmail.com, adam.milczarek@ee.pw.edu.pl, malin@isep.pw.edu.pl*